Available online at www.sciencedirect.com

SciVerse ScienceDirect

Ceramics International 39 (2013) 5485–5493

CERAMICS INTERNATIONAL

www.elsevier.com/locate/ceramint

The preparation of core–shell Al_2O_3/Ni composite powders by electroless plating

Mehmet Uysal*, Ramazan Karslioğlu, Ahmet Alp, Hatem Akbulut

Sakarya University Engineering Faculty, Department of Metallurgical & Materials Engineering, Esentepe Campus, 54187 Sakarya, Turkey

Received 7 November 2012; received in revised form 13 December 2012; accepted 14 December 2012
Available online 4 January 2013

Abstract

Core–shell nanostructured Ni-coated Al_2O_3 composite powders were synthesised by using the electroless plating method. The influence of the chemical components and powder concentration in the Ni coating was investigated by scanning electron microscopy, energy dispersive spectroscopy, and X-ray diffraction techniques. The results show that the concentration of the plating components plays an important role in the formation of core–shell Al_2O_3/Ni composite powders. The nickel content in the composite powders could be effectively controlled by adjusting the nickel chloride content and the concentration of $NaH_2PO_2 \cdot H_2O$ in the plating solution. The nanostructure of the crystalline Ni coatings was observed to be very attractive for achieving good bonding between ceramic particles and matrices for composite production.

Keywords: Electroless Ni coating; Alkaline solution; Core–shell structure; Al_2O_3 powder

1. Introduction

Al_2O_3 has been widely used in many fields due to its good mechanical and anticorrosion properties. However, the utility of a ceramic material in an engineering application is critically determined by its brittleness. Thus, the toughening of ceramic materials is necessary and has been investigated for a long time [1–3]. The wetting process between metals and ceramics is crucial for material joining processes and the production of metal–matrix composites (MMCs). However, a major difficulty found in the liquid–metal processing of composites is the non-wetting nature of ceramics; thus, improved wetting must be achieved to obtain good bonding between a given matrix and corresponding reinforcements. Producing suitable Al_2O_3/metal composite powders is a key step in solving these types of problems. Metal-coated ceramic particles, i.e., particles with a ceramic core and a metallic shell, can improve the wettability between metals and ceramics [4–6].

One type of metal-coated ceramic powder in particular, Al_2O_3/Ni composites, has attracted considerable attention from researchers. In general, metal coatings can be prepared in many ways, such as by chemical vapour–liquid reaction, atomic layer deposition (ALD), spray drying, hydrothermal route, seed-mediated growth precipitation, ball milling, electroless plating. Electroless plating has been recognised as one of the most effective techniques; it is based on the controlled autocatalytic reduction of a metallic salt on a target surface [1,5–7]. Electroless plating has been widely used to prepare protective coatings that are resistant against corrosion and wear effects and improve the wetting of ceramics with metal during melting processes [8–10]. This type of coating, invented in 1946 by Brenner and Riddell [11], has been used in many fields owing to their unique properties [12]. Composite powders prepared by this method show good dispersion, and the metal content in such composites can also be controlled effectively.

The literature reveals some studies related to the coating of Al_2O_3 particle surfaces with Cu [13], Co [14] and Ni [15]. Our work is unique in terms of providing a core–shell layer on Al_2O_3 surfaces by using optimised experimental parameters.

*Corresponding author. Tel.: +90 264 295 57 95, +90 555 422 34 35; fax: +90 264 295 56 01.
E-mail address: mehmetu@sakarya.edu.tr (M. Uysal).

0272-8842/$ - see front matter © 2013 Elsevier Ltd and Techna Group S.r.l. All rights reserved.
http://dx.doi.org/10.1016/j.ceramint.2012.12.060

In this study, we aimed to deposit a very thin layer of Ni on Al_2O_3 particle surfaces by using a $NiCl_2 \cdot 6H_2O$ precursor via the electroless plating method. Because the coating of Ni on ceramic surfaces provides a metal–metal contact for producing strong interfacial bonds between ceramic constituents, a nano-scale core–shell structure seems well-suited to modify the surface chemistry of ceramic components.

2. Experimental

2.1. Pre-treatment process of the Al_2O_3 powders

Before Ni deposition, Al_2O_3 particles with an average size of 60 μm were cleaned and activated. The following process steps were carried out prior to nickel deposition: the Al_2O_3 particles were immersed in an acetone solution for 10 min to clean their surfaces; then, the particles were sensitised in an aqueous solution containing 10 g/l $SnCl_2$ and 30 ml/l HCl; finally, the Al_2O_3 particles were activated in an aqueous solution of 0.25 g/l $PdCl_2$ and 3 ml/l concentrated HCl.

2.2. Electroless nickel plating of Al_2O_3 powders

To deposit a very thin layer of Ni on the Al_2O_3 particle surfaces, the effect of the $NiCl_2$ and Al_2O_3 concentrations in the electrolyte and the sodium hypophosphite (as a reducer) concentration was investigated. These parameters were controlled to obtain a continuous Ni coating with nanostructured grains. Alkaline baths were used for the electroplating process. The composition of the baths and the plating conditions are shown in Table 1. The pH value of the plating solution was controlled continuously during the deposition of Ni. A total plating time of 20 min, a deposition temperature of 70 ± 2 °C and a pH of 8.5 were the conditions chosen for the electroless plating process. After plating, the powder was washed with distilled water and then dried in an incubator at 90 °C. The weight of the Al_2O_3 powders was measured before and after the electroless deposition using an analytical balance with a resolution of 0.0001 g. The weight gain after the deposition process was computed using the formula $\Delta W = W_2 - W_1$, where W_2 is the weight of the Ni-coated powder and W_1 is the weight of the Al_2O_3 powder before coating. The experiments on the Al_2O_3 coating with Ni and the weight change after deposition were repeated several times to optimise the experimental parameters and ensure the reproducibility of the coatings.

Table 1
Composition and operating conditions of the plating bath for Ni coating on Al_2O_3 powders.

Chemical composition of the electroless nickel plating bath and its operating conditions	
$NiCl_2 \cdot 6H_2O$	25.0–75.0 g/l
$C_6H_5NaO_7 \cdot H2O$	120.0 g/l
NH_4Cl	40.0 g/l
$NaH_2PO_2 \cdot H_2O$	4.0, 8.0, 12.0, 16.0 g/l
Powder concentration	5.0, 10.0, 20.0, 40.0 g/l
pH	8, 5
Temperature	70 ± 2 °C
Stirring speed	250 rpm

2.3. Analysis of electroless nickel-coated Al_2O_3 powders

The surface morphology of the shell structure coated on the core Al_2O_3 particles was characterised by an SEM (model JEOL—JSM 6060LV) equipped with an energy dispersive spectroscopy (EDS) attachment. X-ray diffraction (XRD) (model Rigaku D/MAX/2200/PC) analysis was performed on the coated Al_2O_3 particles to determine the possible growth direction and crystallographic characteristics of Ni deposition. The average grain size of the Ni on the Al_2O_3 particles was estimated by XRD using the well-known Scherrer equation.

3. Experimental results and discussions

3.1. The mechanism of formation of core–shell of Al_2O_3/Ni

In electroless nickel plating, active sites are required to initiate the deposition of metallic nickel species. The initiation of electroless nickel deposition is known to be controlled by anodic processes, and the first step involves a non-Faradaic step, namely the adsorption of hypophosphite on the surface of catalyst [16]. The formation mechanism of the core–shell structure of Al_2O_3/Ni is schematically depicted in Fig. 1 and described as follows. Pre-treatment in the $SnCl_2$ solution enhances the adsorption of Pd ions on the surfaces of the Al_2O_3 particles during activation. After sensitisation, Sn^{2+} ions are adsorbed on the surfaces of the Al_2O_3 particles and act as seeds for the formation of Pd nuclei during the activation process, as confirmed by different researchers [17–20]. Specifically, the Sn^{2+} ions react with Pd^{2+} to form uniform Pd catalytic nuclei. The reaction is described as follows:

$$Pd^{2+} + Sn^{2+} \rightarrow Sn^{4+} + Pd^0 \quad (1)$$

Reduced palladium atoms remain on the surface after the sensitisation process. When the activated Al_2O_3 particles are introduced into the electroless nickel plating bath, the following autocatalytic redox reaction occurs:

$$Ni^{2+} + H_2PO_2^- + H_2O \rightarrow H_2PO_3^- + H_2 + Ni^0 \downarrow \quad (2)$$

$$H_2PO^{2-} + H_2O \rightarrow H_2PO_3^- + 2H \quad (3)$$

$$H_2PO^{2-} + H \rightarrow P^0 + OH^- + H_2O \quad (4)$$

Eqs. (2)–(4) indicate that the nickel ions are reduced to metallic nickel, paralleling the oxidation of Pd^0. The reduced nickel particles become electropositive by selectively adsorbing Ni^{2+} in solution because the concentration of Ni^{2+} in the solution is higher than that of $H_2PO_2^-$. This process suppresses nickel from aggregating into large

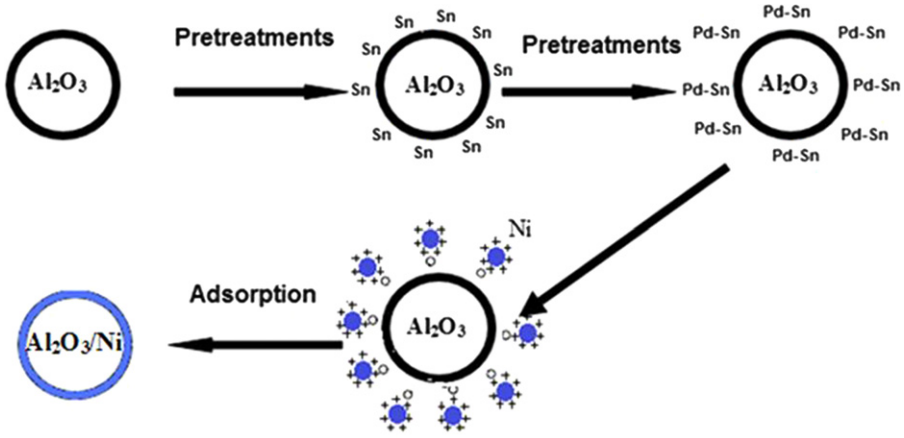

Fig. 1. The mechanism of core–shell of Al_2O_3/Ni by electroless plating.

particles or grains due to the repulsion of like charges [21]. When the charged nickel particles encounter Al_2O_3 particles, it is possible that the Pd catalytic nuclei on the Al_2O_3 powder react with some of the Ni^{2+} ions on nickel particles as described by

$$Pd^0 + Ni^{2+} \rightarrow Pd^{2+} + Ni^0 \quad (5)$$

This reaction indicates that nickel is also reduced by Pd and deposited on the Al_2O_3 surface; then, a nickel-coating layer is formed on the Al_2O_3 particles. Positively charged nickel particles are readily deposited on the surface of Al_2O_3. When the surface of Al_2O_3 is fully coated, Al_2O_3 becomes electropositive. Meanwhile, the reduced nickel particles are also electropositive. Due to the repulsion of these like charges, no other nickel particles are deposited on the surface of Al_2O_3. Finally, a quasi-single-particle nickel layer is formed on the surface of Al_2O_3 [21]. Thus, Al_2O_3–nickel core–shell structures are obtained.

3.2. The influence of processing parameters on core–shell structures

Before depositing Ni on the Al_2O_3 surfaces, we carried out several electroless coating experiments to optimise the pH value and bath temperature of the electrolyte. We determined that the core–shell structure could only be obtained at a pH value of 8.5 and a temperature of 70 °C, conditions that initiate the decomposition and nano-scale nucleation of Ni from $NiCl_2 \cdot 6H_2O$.

The Al_2O_3 particles were coated with Ni using different $NiCl_2 \cdot 6H_2O$ contents in the electrolyte. Fig. 2 shows the influence of the $NiCl_2$ content in the plating solution on the deposited Ni content in the produced Al_2O_3/Ni powders. The figure indicates that the weight gain increased with the increase in the $NiCl_2 \cdot 6H_2O$ content. This suggests that the Ni content on the Al_2O_3 powder surfaces can be controlled by controlling the concentration of $NiCl_2 \cdot 6H_2O$. Wang et al. [5] studied Cu-coated Al_2O_3 composite powders using the electroless plating method. They found that the weight of the powders increased with

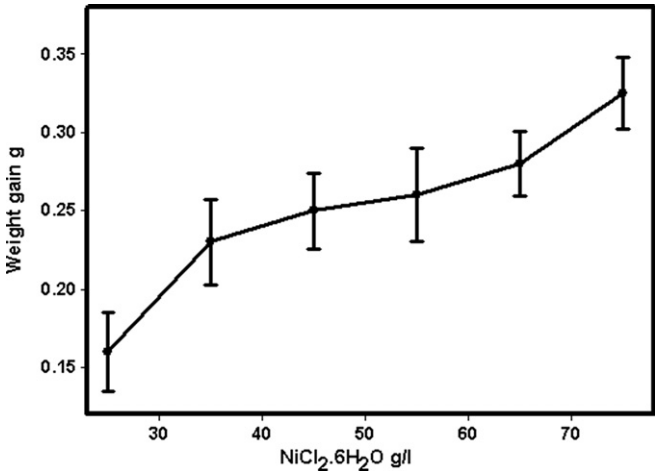

Fig. 2. Effect of the $NiCl_2 \cdot 6H_2O$ content in the bath solution on the weight increment in Ni coated composite powders.

the increase in the $CuSO_4 \cdot 5H_2O$ content. It can be concluded that if the coating homogeneity and continuity can be controlled for all precursor additions, increasing the $NiCl_2 \cdot 6H_2O$ content can control the coating thickness of Ni on ceramic surfaces.

Eq. (2) shows that high concentrations of $NaH_2PO_2 \cdot H_2O$ can increase the driving force of reaction and thus increase the plating speed. However, the reaction speed is also controlled by the concentration of $NiCl_2$, reductive material conditions, and pH, among other factors. In our experiments, the initial pH value and the concentration of $NiCl_2$ were fixed. When the $NaH_2PO_2 \cdot H_2O$ content in the bath solution is low, the reduction reaction is controlled by a reductive material of $NaH_2PO_2 \cdot H_2O$ for kinetic reasons. An increase in the concentration of $NaH_2PO_2 \cdot H_2O$ will generate more electrons; therefore, the reaction speed increases.

Fig. 3 shows the effect of the sodium hypophosphite concentration on the weight gain of the Al_2O_3 particles and composition of the core–shell structures. As can be clearly seen, the phosphorous content in the deposits increases

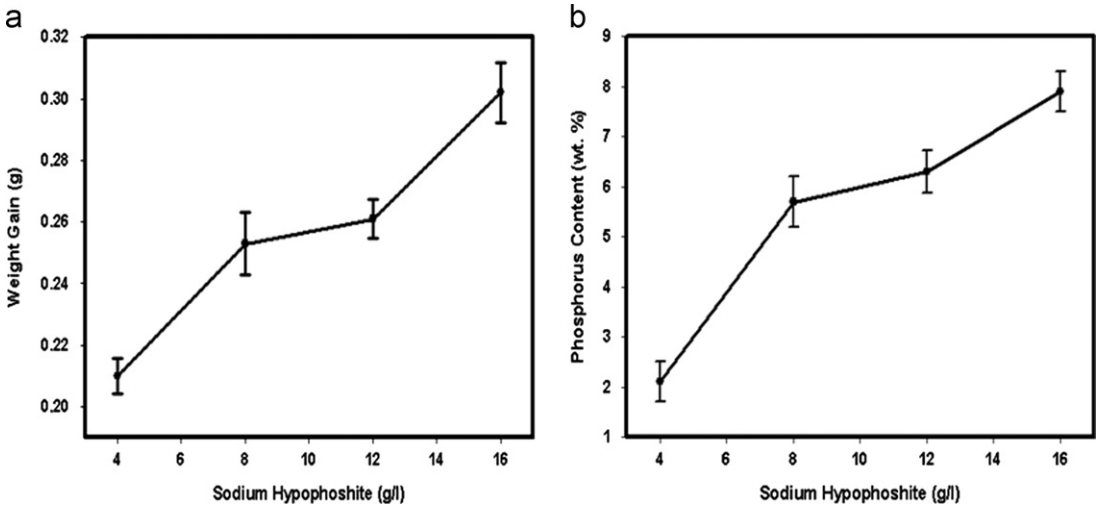

Fig. 3. Effect of the $NaH_2PO_2 \cdot H_2O$ content in Ni coated composite powders on (a) the weight gain and (b) phosphorus content.

slightly and almost linearly with the increase in the $NaH_2PO_2 \cdot H_2O$ concentration. This is because even though the number of electrons available for metal ion reduction increases with an increase in the concentration of sodium hypophosphite, the rate at which the metal ions are made available is limited by the amount of complexing agent present in the bath [22]. It has also been shown that sodium hypophosphite is the dominant factor in the electroless plating process. For instance, Pang et al. [23] proved that increasing the $NaH_2PO_2 \cdot H_2O$ concentration in a plating bath results in an increase in the phosphorus content of the deposit.

As shown in Fig. 3, the weight gain increases with the concentration of $NaH_2PO_2 \cdot H_2O$ as well; this yields a more uniform powder. As the concentration of $NaH_2PO_2 \cdot H_2O$ increases, the oxidation speed increases, and thereby, the plating speed increases. This may be explained by the fact that during the electroless plating process, the overall reaction described by Eq. (2) occurs.

According to this chemical reaction, increasing the concentration of $NaH_2PO_2 \cdot H_2O$ can lead to an increase in the oxidation rate of hypophosphite, which in turn accelerates the plating rate and increases the driving force of reaction.

Fig. 4 shows SEM images of the Al_2O_3/Ni composite particles obtained with different $NaH_2PO_2 \cdot H_2O$ concentrations. To determine the effect of the $NaH_2PO_2 \cdot H_2O$ concentration, the Al_2O_3 particle loading in the electrolyte was held constant at 10 g/l. Fig. 4 shows that the size of the Ni deposits increased with the increase in the concentration of $NaH_2PO_2 \cdot H_2O$ in the electrolyte. Meanwhile, the uniformity of the coating was improved up to a certain $NaH_2PO_2 \cdot H_2O$ concentration. When 4 g/l $NaH_2PO_2 \cdot H_2O$ was added, very fine Ni grains were observed on the Al_2O_3 surfaces. Dense nano-structures were obtained on the Al_2O_3 particle surfaces, producing an Al_2O_3–Ni core–shell structure. However, the coatings were neither continuous nor homogeneous. This was due to the poor reduction of Ni ions due to the lack of a reducing agent. Increasing the $NaH_2PO_2 \cdot H_2O$ concentration to 12 g/l resulted in a very continuous, dense and full coverage of the Al_2O_3 particle surfaces. Further increasing the $NaH_2PO_2 \cdot H_2O$ content to 16 g/l in the electrolyte produced very large grains and reduced the homogeneity of the core–shell structure. Increasing the $NaH_2PO_2 \cdot H_2O$ content also led to a large grain size distribution, and large grains were observed to grow on the single-layer core–shell-structured Ni. Similar results were reported by Zhang et al. [24] for the electroless coating of Co on nano-scale Al_2O_3 surfaces. They reported that the average size of deposited Co particles was larger when prepared at a high $NaH_2PO_2 \cdot H_2O$ content; moreover, the uniformity was also reported to improve. The appearance of larger particles is likely explained by two factors: (i) the presence of larger particles among the initial particles and (ii) the agglomeration of large particles and several small particles after electroless plating.

In Fig. 5, the grain sizes of the electroless nickel coatings on the Al_2O_3 particles are shown as a function of the reducer content and powder load in the plating bath. Fig. 5a shows the relationship between the grain size and reducer content, whereas Fig. 5b shows that between the grain size and powder load. The average grain size of the Ni on the Al_2O_3 particles was estimated by the XRD method using the well-known Scherrer equation. As shown in Fig. 5a, increasing the amount of reducer led to an increase in the grain size of the Ni on the Al_2O_3 particles, whereas Fig. 5b shows that an increase in the powder load caused a decrease in the grain size. The electroless reaction proceeded around the Pd catalyst, after which Ni was continuously deposited on the catalyst. Ultimately, a continuous nickel layer was obtained when nickel particles grew to connect. Hence, the electroless plating time increased with the $NaH_2PO_2 \cdot H_2O$ concentration, resulting in the formation of nickel particles with large grain sizes. However, increasing the Al_2O_3 concentration resulted in

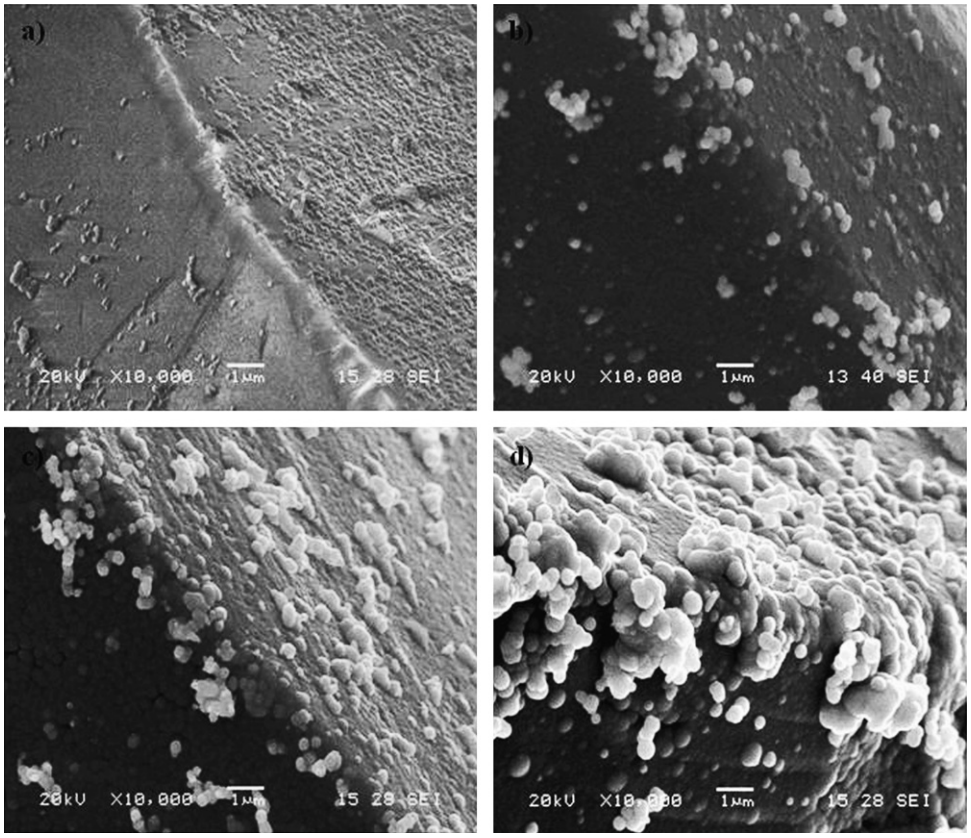

Fig. 4. SEM images of Al_2O_3/Ni composite powders with different $NaH_2PO_2 \cdot H_2O$ in the electrolyte; (a) 4 g/l $NaH_2PO_2 \cdot H_2O$, (b) 8 g/l $NaH_2PO_2 \cdot H_2O$, (c) 12 g/l $NaH_2PO_2 \cdot H_2O$ and (d) 16 g/l $NaH_2PO_2 \cdot H_2O$.

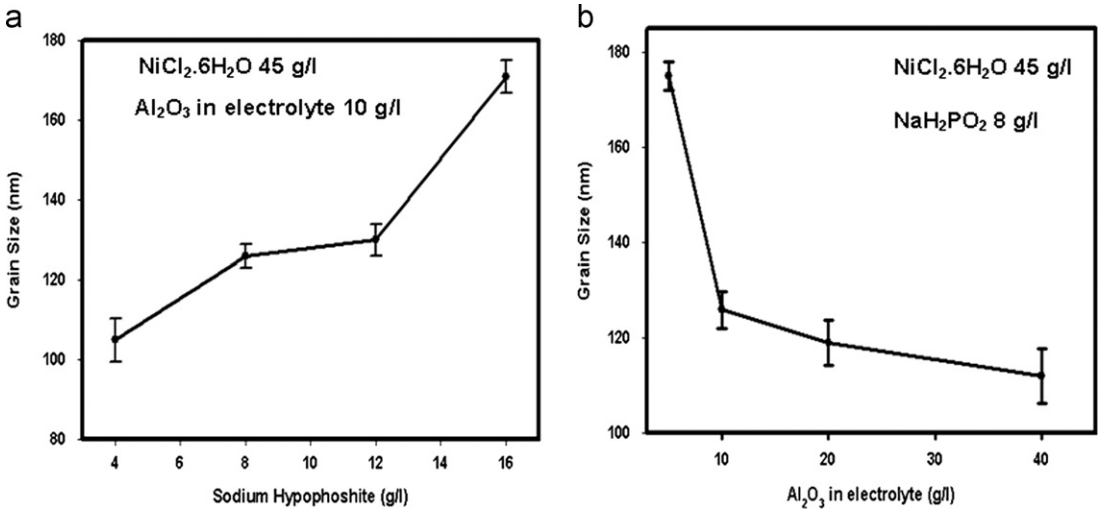

Fig. 5. The relationship between deposited Ni grain size: (a) reducer content and (b) powder loading.

an increase in the concentration of the Pd catalyst in the whole system. Because the $NiCl_2$ concentration was held constant, increasing the number of electroless reaction sites rapidly reduced the Ni^{2+} concentration on the surface of Al_2O_3, resulting in a decrease in the grain size of the nickel particles. It was expected that the different amounts of Al_2O_3 powder added could result in variable Ni contents on every particle surface. Fig. 6 shows the effect of the alumina powder concentration in the electrolyte on the Ni deposited layer.

SEM micrographs of Al_2O_3 surface-coated samples produced with different Al_2O_3 concentrations in the electrolyte are shown in Fig. 6. Some Ni precipitates are observed on the surface of the coated powders when the

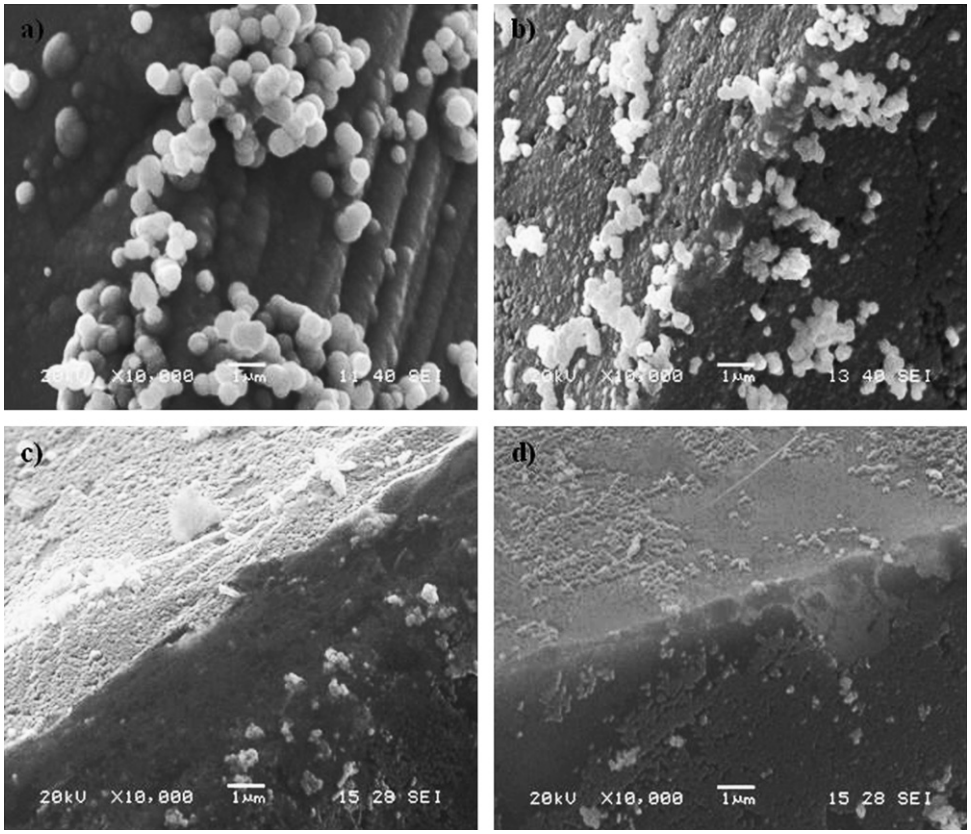

Fig. 6. SEM image of the powder with different particle loadings into electrolyte; (a) 5 g/l, (b) 10 g/l, (c) 20 g/l, and (d) 40 g/l.

Al_2O_3 particle loading was 5 g/l. The precipitates occur as small, light-coloured spheres in Fig. 6a. A similar observation was reported by Palaniappa et al. [25] for the nickel plating of graphite powders when a low concentration of graphite in the electrolyte was used.

As is clearly shown in Fig. 6b, nearly full coverage of the Al_2O_3 surfaces with a thin layer of Ni was achieved by the addition of 10 g/l Al_2O_3 particles to the electrolyte. The density of the Ni layer deposited on the Al_2O_3 surfaces was observed to be more uniform for the addition of 10 g/l Al_2O_3 to the electrolyte than that for the addition of 5 g/l Al_2O_3. This was attributed to the higher amount of Ni ions that can be reduced on the Al_2O_3 surfaces because the Ni ion concentration was held constant in the plating bath when the particle concentration was high. Another possible reason for this increase in the uniformity of Ni deposition could be the heterogeneous nucleation effect induced at a high particle concentration due to an increase in the surface area and thus the number of nucleation sites on the Al_2O_3 particle surfaces. The size of the deposited Ni grains and the thickness of the Ni layer were both found to decrease with an increase in the particle concentration in the electrolyte, as shown in Fig. 6c and d. These effects were observed to result in the production of finer Ni particles on the surfaces and thinner layer thicknesses, as well as a decrease in the size of the Ni spheres resulting from the heterogeneous nucleation effect due to the large number of available nucleation sites on the ceramic surfaces. Moreover, increasing the particle loading in the electrolyte resulted in inhomogeneous coating on the ceramic surfaces and the discontinuity of the Ni shell. This suggests that the precursor and reducer contents should be increased when the particle content is increased beyond 10 g/l in the electrolyte.

It can be further understood from the XRD patterns shown in Fig. 7 that the Ni content in the surface coatings decreased with the increase in the powder concentration in solution. Therefore, the Ni–P content in the composite powder can be varied by controlling the amount of powder loaded into the bath, where a higher powder load results in a lower nickel content on the powder surface (see Fig. 7, nickel peaks at approximately $2\theta = 45^\circ$).

3.3. Optimum process parameters for nano-scale core–shell structures

A very thin layer of Ni fully covering the surfaces of Al_2O_3 particles was achieved with a grain size between 105 and 175 nm, obtained at specific reducer and particle contents. We were primarily focused on the continuous deposition of Ni to form core–shell structures. $NaH_2PO_2 \cdot H_2O$ and Al_2O_3 particle contents of 8.0 g/l and 10 g/l, respectively, in the electrolyte were considered the optimum process parameters for coating 60 μm Al_2O_3 particles.

Fig. 8a and b demonstrate the microstructures of the uncoated and coated Al_2O_3 particles with core–shell structures, respectively. The SEM image shown in Fig. 8b indicates that a homogeneous and uniform nickel shell was deposited on the Al_2O_3 particles. The high-magnification SEM image in Fig. 8c shows nano-sized Ni grains on the Al_2O_3 surfaces with a dense and continuous coating structure. EDS was performed to analyse the structure of the plated powders with a core–shell structure; the results are presented in Fig. 8d. The figure shows that Ni, P, O and Al were present in the structure. Thus, the powder produced was considered to be composed of Al_2O_3 and Ni–P. The grain size of the Ni core–shell structures synthesised under the optimum process parameters of 8.0 g/l $NaH_2PO_2 \cdot H_2O$ and 10 g/l Al_2O_3 particles in the electrolyte using a precursor of 45 g/l $NiCl_2 \cdot 6H_2O$ was calculated to be 128 nm.

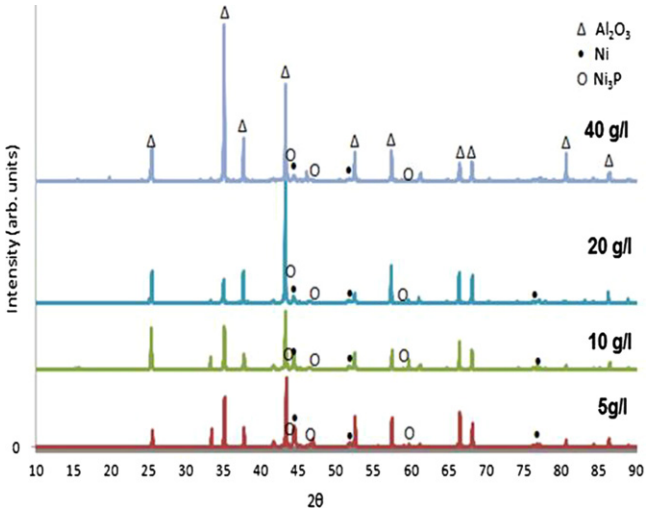

Fig. 7. XRD pattern of the powder with different loads.

For greater detail, higher-magnification images of the electroless-nickel-coated Al_2O_3 surfaces with two different $NaH_2PO_2 \cdot H_2O$ contents of 4.0 and 8.0 g/l at a constant particle content in the electrolyte (10 g/l) are presented in Fig. 9. Fig. 9a shows a few uncoated regions on the particle surfaces that occurred because of the insufficient amount of Ni ions in the electrolyte. The micrograph in Fig. 8b shows that the Al_2O_3 powder surfaces were fully coated with a nano-sized EN coating that was dense and uniform throughout the surface of the particles. Fig. 9 also indicates that no preferential nucleation or growth was observed on the Al_2O_3 surfaces, which has previously been observed on electroless-Ni-coated SiC surfaces. Indeed, this preferential direction was observed to occur over convex areas of SiC surfaces [26].

The XRD patterns obtained for the original ceramic powder and Al_2O_3/nickel core–shell structures are shown

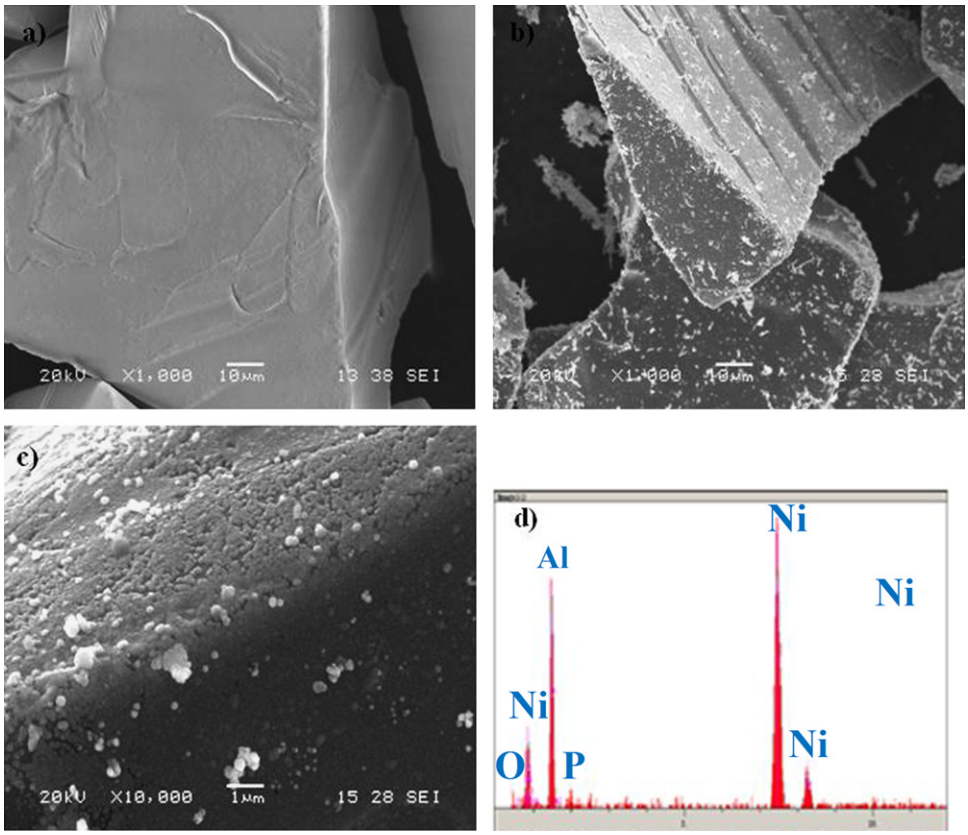

Fig. 8. SEM image of (a) uncoated Al_2O_3, (b) Al_2O_3/Ni core–shell structure, (c) high magnification image of Al_2O_3/Ni core–shell structure, and (d) EDS spectrum of the Ni coated Al_2O_3.

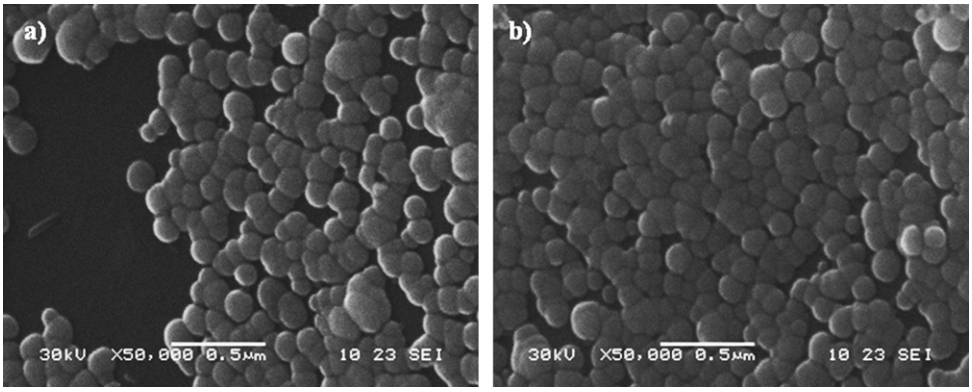

Fig. 9. High magnification Ni coating SEM micrographs on Al_2O_3 surfaces with a constant particle content in the electrolyte of 10 g/l: (a) 4.0 g/l $NaH_2PO_2 \cdot H_2O$ and (b) 8.0 g/l $NaH_2PO_2 \cdot H_2O$ content.

in Fig. 10. As seen from the XRD pattern in Fig. 10, the deposited Ni produces sharp diffraction patterns because of the crystallinity of the nickel deposited on the Al_2O_3 surfaces.

As it is well known, coating ceramic particles with a metallic layer always promotes wetting between the reinforcement phases and the metallic matrix of MMC materials. The metallic surface layer on these ceramics contributes to interfacial bonding between the constituents of such composites. Increasing the coating thickness on the reinforcement surface sometimes results in the degradation of the matrix and/or reinforcement due to excessive reaction at the interfaces. Thus, coating a thin layer of Ni on Al_2O_3 particles to produce nano-sized core–shell structures will not only provide good interfacial bonding but also allow for low-temperature sintering due to the high reactivity of nano-sized grains, owing to their high surface area.

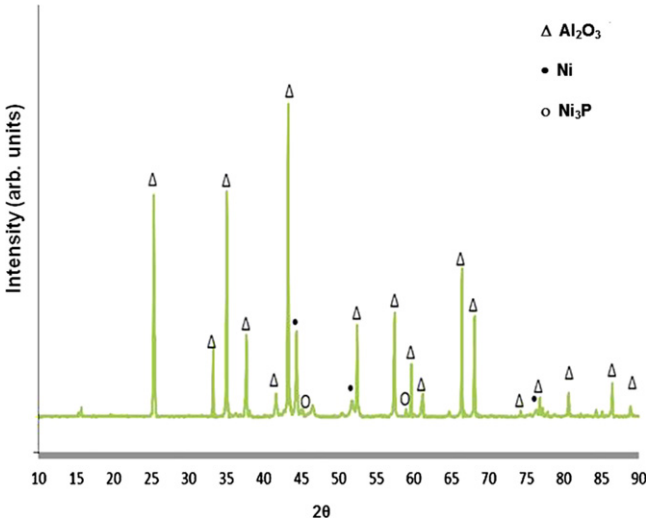

Fig. 10. XRD pattern of the core–shell Al_2O_3/Ni composite powders 8.0 g/l $NaH_2PO_2 \cdot H_2O$ content and 10 g/l Al_2O_3.

4. Conclusions

The surfaces of Al_2O_3 ceramic powder particles were successfully coated by using a $NiCl_2 \cdot 6H_2O$ precursor through the electroless plating method. The experimental findings reveal that coating a thin shell (nickel) on core ceramic particle (Al_2O_3) surfaces is strongly dependent on the concentration of the plating components. The content and the grain size of nickel in the composite powders can be controlled by the nickel chloride content and the concentration of $NaH_2PO_2 \cdot H_2O$ in the plating solution.

The Ni layer coating the Al_2O_3 particles was controlled by the $NiCl_2 \cdot 6H_2O$ content. The following main conclusions can be drawn from the present study:

1. A Ni layer was deposited on the surfaces of Al_2O_3 particles by an electroless coating technique. The layer showed a relatively continuous and uniform structure, with a grain size of 60 μm. Increasing the $NiCl_2 \cdot 6H_2O$ content resulted in an increase in the weight gain of the powders because of the corresponding enhancement in the extent of electroless Ni deposition on the ceramic surfaces.
2. The grain size of Ni on the Al_2O_3 particle surfaces after electroless deposition was detected to vary between 105 and 175 nm, depending on the $NaH_2PO_2 \cdot H_2O$ concentration and the particle content in the electrolyte.
3. Increasing the concentration of $NaH_2PO_2 \cdot H_2O$ resulted in the deposition of coarser Ni grains (i.e., a thicker coating layer) on the Al_2O_3 surfaces, whereas increasing the particle content in the electrolyte produced finer grains (i.e., a thinner coating layer) on the Al_2O_3 surfaces.
4. The optimum process parameters for coating the Al_2O_3 surfaces with a Ni shell were determined to be 8.0 g/l $NaH_2PO_2 \cdot H_2O$ and 10 g/l Al_2O_3 particles in the electrolyte using a precursor of 45 g/l $NiCl_2 \cdot 6H_2O$.
5. The present study shows that the formation of core–shell structures by alkaline electroless coating can be a useful method for producing Al_2O_3-reinforced composites without deteriorating the interfaces between components.

References

[1] L. Guo-jun, X. Huang, J. Guo, Fabrication of Ni-coated Al_2O_3 powders by the heterogeneous precipitation method, Materials Research Bulletin 36 (2001) 1307–1315.

[2] G. Xiao-xian, X. Huang, J. Guo, D. Chena, Ni-coated Al_2O_3 powders, Ceramics International 28 (2002) 623–626.
[3] S.C. Hanyaloglu, B. Aksakal, I.J. McColm, Reactive sintering of electroless nickel-plated aluminum powders, Materials Characterization 47 (2001) 9–16.
[4] E.A. Aguilar, C.A. Leon, A. Contreras, V.H. López, R.A.L. Drew, E. Bedoll, Wettability and phase formation in TiC/Al-alloys assemblies, Composites Part A 33 (2002) 1425–1428.
[5] H. Wang, J. Jia, H. Song, X. Hu, H. Sun, D. Yang, The preparation of Cu-coated Al_2O_3 composite powders by electroless plating, Ceramics International 37 (2011) 2181–2184.
[6] J. Dai, X. Liu, H. Zhai, Z. Liu, J. Tian, Preparation of Ni-coated Si_3N_4 powders via electroless plating method, Ceramics International 35 (2009) 3407–3410.
[7] H. Beygi, H. Vafaeenezhad, S.A. Sajjadi, Modeling the electroless nickel deposition on aluminum nanoparticles, Applied Surface Science 258 (2012) 7744–7750.
[8] G.P. Ling, Y. Li, Influencing factors on the uniformity of copper coated nano-Al_2O_3 powders prepared by electroless plating, Materials Letters 59 (2005) 1610–1613.
[9] G. Shi, J. Han, Z. Zhang, H. Song, B.Taek Lee, Pretreatment effect on the synthesis of Ag-coated Al_2O_3 powders by electroless deposition process, Surface and Coatings Technology 195 (2005) 333–337.
[10] C.A. Leon, R.A.L. Drew, The influence of nickel coating on the wettability of aluminum on ceramics, Composites Part A 33 (2002) 1429–1432.
[11] K.G. Keong, W. Sha, S. Malinov, Crystallisation kinetics and phase transformation behaviour of electroless nickel–phosphorus deposits with high phosphorus content, Journal of Alloys and Compounds 334 (2002) 192–199.
[12] Z. Gui-Zhen, C. Mao-Sheng, Z. Liang, J. Hai-Bo, X. Hui, W. Zheng-Ping, Preparation and dielectric enhancement of nickel-coated β SiC nanoparticles, Journal of Inorganic Materials 21 (2006) 797–802.
[13] W.H. Lin, H.F. Chang, Effect of chelating agents on the structure of electroless copper coating on alumina powder, Surface and Coatings Technology 107 (1998) 48–54.
[14] Y. Huang, K. Shi, Z. Liao, Y. Wang, L. Wang, F. Zhu, Studies of electroless Ni–Co–P ternary alloy on glass fibers, Materials Letters 61 (2007) 1742–1746.
[15] Z. Guizhen, C. Maosheng, H. Lin, H. Jin, Y. Kang, Y. Chen, Nickel layer deposition on SiC nanoparticles by simple electroless plating and its dielectric behaviors, Powder Technology 168 (2006) 84–88.
[16] D. Hongbin, L. Hongxi, W. Fuhui Electroless, Ni–P coating preparation of conductive mica powder by a modified activation process, Applied Surface Science 253 (2006) 2474–2480.
[17] H. Xu, Y.Z. Kang, L. Zhang, H.B. Jin, B. Wen, B.L. Wen, J. Yuan., M.S. Cao, Deposition behavior and mechanism of Ni nanoparticles on surface of SiC particles in solution systems, Chinese Physics Letters 27 (5) (2010) 058103.
[18] Y.Q. Kang, M.S. Cao, J. Yuan, L. Zhang, B. Wen, X.Y. Fang, Preparation and microwave absorption properties of basalt fiber/nickel core–shell heterostructures, Journal of Alloys and Compounds 495 (2010) 254–259.
[19] G.Z. Zou, M.S. Cao, L. Zhang, J.G. Li, H. Xu, Y.J. Chen, A nanoscale core-shell of β-SiC_P–Ni prepared by electroless plating at lower temperature, Surface and Coatings Technology 201 (2006) 108–112.
[20] Y.Q. Kang, M.S. Cao, J. Yuan, X.Y. Fang, Orientation-dependent electromagnetic properties of basalt fibre/nickel core shell heterostructures, Chinese Physics B 19 (1) (2010) 017701.
[21] Y.J. Chen, M.S. Cao, Q. Xu, J. Zhu, Electroless nickel plating on silicon carbide nanoparticles, Surface and Coatings Technology 172 (2003) 90–94.
[22] T.S.N. Sankara Narayanan, S. Selvakumar, A. Stephen, Electroless Ni–Co–P ternary alloy deposits: preparation and characteristics, Surface and Coatings Technology 172 (2003) 298–307.
[23] J. Pang, Q. Li, W. Wang, X. Xu, J. Zhai, Preparation and characterization of electroless Ni–Co–P ternary alloy on fly ash cenospheres, Surface and Coatings Technology 205 (2011) 4237–4242.
[24] C. Zhang, G.P. Ling, J.H. He, Co–Al_2O_3 nanocomposites powder prepared by electroless plating, Materials Letters 58 (2003) 200–204.
[25] M. Palaniappa, G. Veera Babu, K. Balasubramanian, Electroless nickel–phosphorus plating on graphite powder, Materials Science and Engineering A 471 (2007) 165–168.
[26] M. Uysal, R. Karslioglu, A. Alp, H. Akbulut, Nanostructured core–shell Ni deposition on SiC particles by alkaline electroless coating, Applied Surface Science 257 (2011) 10601–10606.